J Solid State Electrochem (2010) 14:263–270
DOI 10.1007/s10008-009-0960-9

ORIGINAL PAPER

Spectroelectrochemical characteristics of poly(3,4-ethylenedioxythiophene)/iron hexacyanoferrate film-modified electrodes

Andrzej P. Nowak · Monika Wilamowska · Anna Lisowska-Oleksiak

Received: 30 December 2008 / Revised: 9 March 2009 / Accepted: 31 March 2009 / Published online: 27 October 2009
© Springer-Verlag 2009

Abstract Spectroelectrochemical measurements of poly (3,4-ethylenedioxythiophene) (pEDOT) modified by iron hexacyanoferrate (Fehcf) network, chloride (Cl), polystyrenesulfonate (PSS), and hexacyanoferrate (FeCN) ions were shown. Depending on the electrode potential, three main maxima absorbance were recorded. The first related to, the π–π* transition in undoped state of pEDOT, the second and the third are ascribed to transitions between the valence band and the polaron and bipolaron bands, respectively. There is also identified spectrophotometric response from the ligand–metal charge transfer of hexacyanoferrates from pEDOT modified with Fehcf and FeCN. The energy band gap (E_g) was evaluated from the spectroelectrochemical curves of the undoped pEDOT films. The pEDOT/Fehcf material exhibits the band gap of 1.40 eV which is the lowest among measured E_g values equal 1.55, 1.53, and 1.58 eV for pEDOT/FeCN, pEDOT/Cl, and pEDOT/PSS, respectively. Thus, synergetic effect of polymer and Prussian blue is proved as a significant decrease of the E_g value.

Keywords Poly(3,4-ethylenedioxythiophene) · Prussian blue · Spectroelectrochemistry · UV-Vis · Energy band gap

Introduction

In the last 30 years, conducting polymers with π-conjugated electronic structures have been widely investigated due to their potential industrial applications based on their high conductivity and good environmental stability [1–4]. Among these polymers, poly(3,4-ethylenedioxythiophene) (pEDOT) has received considerable attention [4–6], firstly, because of the low oxidation potential of pEDOT and secondly, due to its stability in the oxidized form which makes it suitable for different applications [1, 7, 8].

There are known attempts to insert organic or inorganic materials into conducting polymers matrix [9–12]. Inserted materials can counterbalance electrostatic charge of the polymer chain. The anions can be immersed into the polymer by ion exchange caused by nature of the conducting polymer. One may expect that induction of the new electronic properties of the polymer is caused by inserted component [3, 9, 13].

Interest has been focused on the polynuclear transition metal hexacyanometallates due to their electronic, electrochemical, and spectrophotometric properties [14–18]. The most popular metal hexacyanometallate used as a dopant or an inorganic conductor for modified electrodes with electronically conducting polymers is iron hexacyanoferrate [11, 12]. Randriamahazaka et al. claim that for layer-by-layer material poly(3,4-ethylenedioxythiophene)/iron hexacyanoferrate (pEDOT/Fehcf), cooperative effect (synergy) is observed within such composite [12]. This is reflected by increase of faradaic and capacitive responses of pEDOT in acetonitrile and water solutions in the presence of Fehcf [12, 19].

It is known that optical properties of the material depend on the nature of the polymer and its dopants [20–22]. In situ ultraviolet-visible (UV-Vis) spectroscopy allows observing electronic changes taking place in the material during electrochemical reactions. In this work, the goal is to determine an influence of the type component on an electronic stage of the hybrid system. Especially, we have

A. P. Nowak · M. Wilamowska · A. Lisowska-Oleksiak (✉)
Department of Chemical Technology, Chemical Faculty,
Gdansk University of Technology,
Narutowicza 11/12,
80-233 Gdansk, Poland
e-mail: alo@pg.gda.pl

focused on the electronic properties of the pEDOT modified with iron hexacyanoferrate and a synergy effect measured as an energy band gap.

Experimental

Chemicals

Monomer 3,4-ethylenedioxythiophene (EDOT) and inorganic compounds: $K_4Fe(CN)_6$, $K_3Fe(CN)_6$, KCl were supplied by Fluka-Aldrich; $FeCl_3$ anhydrous were supplied by Riedel-de Haën, Germany and poly(sodium 4-styrenesulfonate) (M.W. CA. 70000) supplied by Aldrich. All chemicals were of analytical grade and used without further purification. Aqueous electrolytes used for the synthesis of the materials were prepared using triply distilled water.

Experimental procedures and instrumentation

Three-electrode one-compartment cell was used to obtain polymer films. An indium–tin oxide (ITO)-coated glass (~1.0 cm^2, surface resistance 40 Ω/cm^2) served as a working substrate electrode. Platinum mesh (10 cm^2) was used as a counter electrode, and Ag/AgCl in 0.1 M KCl served as a reference electrode. The polymer films were obtained by an anodic polarization at the potential E=0.9 V (each case) from an aqueous solution containing monomer EDOT (0.015 M) and different electrolytes for each material: (1) $K_4Fe(CN)_6$ and $K_3Fe(CN)_6$ (concentrations of the salts in the limits from 0.1 mM to 1.0 M according to Polish Patent Application [23]) for pEDOT with hexacyanoferrates counterions (pEDOT/FeCN), (2) 0.1 M KCl for pEDOT with chloride counterions (pEDOT/Cl), and (3) 0.1 M PSSNa for pEDOT with polystyrenesulfonate counterions (pEDOT/PSS). The total charge during electropolymerization was 0.9 C/cm^2 for pEDOT/FeCN. In case of pEDOT/PSS and pEDOT/Cl film, the total charge during polymerization was 40 mC/cm^2.

The pEDOT modified with iron hexacyanoferrate (pEDOT/Fehcf) was prepared by a multicyclic polarization of the pEDOT/FeCN film in the freshly prepared $FeCl_3$ aqueous electrolyte (pH 2.5) [24]. During the subsequent potentiodynamic polarization (sweep rate, 20 mV/s; 60 cycles), at the potential range from −0.25 to 0.8 V hexacyanoferrate ions from pEDOT/FeCN react with $Fe^{3+/2+}$ from the solution, and iron hexacyanoferrate is formed in the polymer matrix. Generic reaction of inorganic redox network Fehcf formation could be presented as follows [24]: $y\mathrm{Fe(CN)}_6^{3-/4-} + x\mathrm{Fe}^{\mathrm{II/III}} \rightarrow \mathrm{Fe}_x^{\mathrm{II/III}}\left[\mathrm{Fe}^{\mathrm{II/III}}(\mathrm{CN})_6\right]_y$. The number of cycles represents steady state condition of the ion sorption/desorption process. After preparation, samples were rinsed using triply distilled water and used in the spectroelectrochemical measurements.

In situ spectroelectrochemical measurements were performed in the quartz-deaerated cell with 0.1 M KCl aqueous electrolyte. The quartz cuvette served as three-electrode one-compartment electrochemical cell (Fig. 1). Absorbance was measured between 350 and 1100 nm at a constant potential while stable current was achieved (i=const.). The potential was changed from +0.7 V to −1.1 V with 0.1 V potential step for each UV-Vis scan. The electrode ITO in the reference cuvette was not polarized as the absorbance intensity of ITO does not change during polarization.

All electrochemical experiments were performed using the potentionstat–galvanostat system AutoLab PGStat10. Computer-controlled spectroelectrochemical measurements were performed using UNICAM UV 300 spectrometer (Thermo Fisher Scientific Inc., USA), and for potential step polarization AutoLab PGStat 10, GPES 4.9 was used. Instrumentation setup is presented in Fig. 1.

Mathematical analysis of the UV-Vis spectra was performed by program GRAMS/32 (Galactic Industries Corporation, Salem, USA).

Results and discussion

ITO/pEDOT/FeCN

Figure 2a (I) shows UV-Vis spectra of pEDOT/FeCN. Depending on the potential, the three maxima can be seen: B, C, and D. There is also a hump A below 400 nm

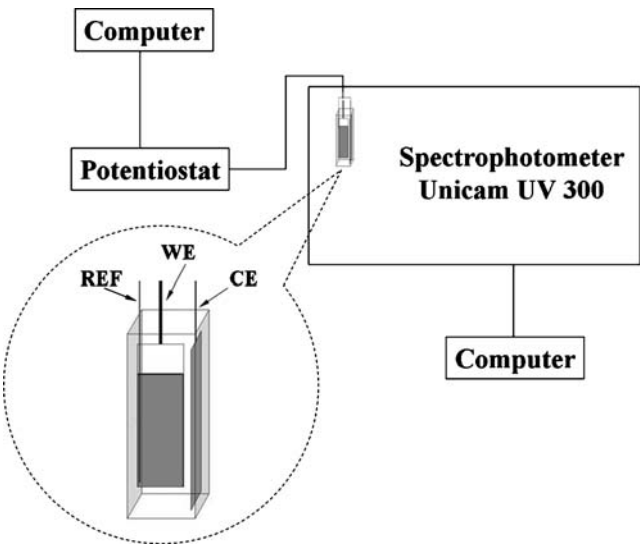

Fig. 1 The instrumentation setup for the spectroelectrochemical measurements; *WE* working electrode (ITO coated glass), *REF* reference electrode (Ag/AgCl), *CE* counter electrode (platinum plate ~2.5 cm^2); outer electrolyte, 0.1 M KCl

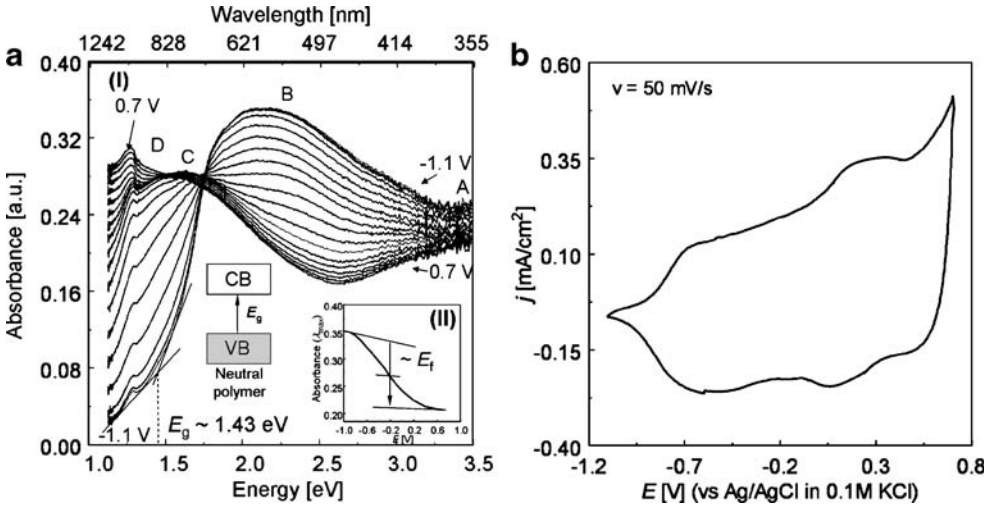

Fig. 2 **a** (*I*) UV-Vis spectra for pEDOT/FeCN film in 0.1 M KCl; potential range from –0.9 to 0.7 V, inset (*II*) shows absorbance vs. potential spectra. **b** Cyclic voltammetry curves obtained for ITO/pEDOT/FeCN electrode in 0.1 M KCl solutions; sweep rate, 50 mV/s

absorbance of which is slightly decreasing with the cathodic polarization. It is known that ligand metal charge transfer (LMCT; $^2T_{1g} \rightarrow {}^2T_{2g}$) for $Fe(CN)_6^{3-}/Fe(CN)_6^{4-}$ system in aqueous solution as well as for pure solid Fehcf are seen at λ_{max}=420 nm only for oxidized form [25–27]. LMCT for $Fe(CN)_6^{4-}$ as well is known to occur at λ_{max}= 323 nm [28]. Thus, we may only suppose that rising part of the spectra (A) below 400 nm is very likely to be related to LMCT for both $Fe(CN)_6^{3-}$ and $Fe(CN)_6^{4-}$ complex. The signal on the spectra for $Fe(CN)^{3-}$ and $Fe(CN)^{4-}$ LMCT are very likely to overlap each other to the extent that the identification of separate valence states is not possible.

Figure 2b shows cyclic voltammetry curve obtained for ITO/pEDOT/FeCN electrode. The electrode activity at potential $E \approx 0.20$ V is ascribed to $Fe(CN)_6^{3-}/Fe(CN)_6^{4-}$ redox couple in the polymer matrix.

In the neutral state (E=−0.9 V), polymer exhibits maximum absorption B at $\lambda_{max} \approx 598$ nm. Comparing with literature data, the maximum B is ascribed to the π–π* transition in the undoped pEDOT film [29–33] or in terms of solid state chemistry, the π–π* transition is interpreted as valence band to conduction band [34]. Upon doping, the π–π* transition decreases at the expense of broad maximum absorption above 700 nm which is associated with transition from valance band to polaron band (λ_{max}C). Further anodic polarization, E>0.3 V, causes the transformation of the doped phase into the new phase known as "overdoped" (λ_{max}D) [4]. This band has been assigned to the evolution of bipolaron states within the polymer film [4, 6].

The energy band gap, E_g, calculated from the onset of the π-π* transition is equal 1.55 eV which varies from the values reported for other pEDOT composites e.g. pEDOT/PAMS (1.65 eV) [33].

From the absorbance vs. potential data at λ_{max}B, it is possible to determine the polymer formal potential (E_f) where there is 50% neutral polymer and 50% oxidized

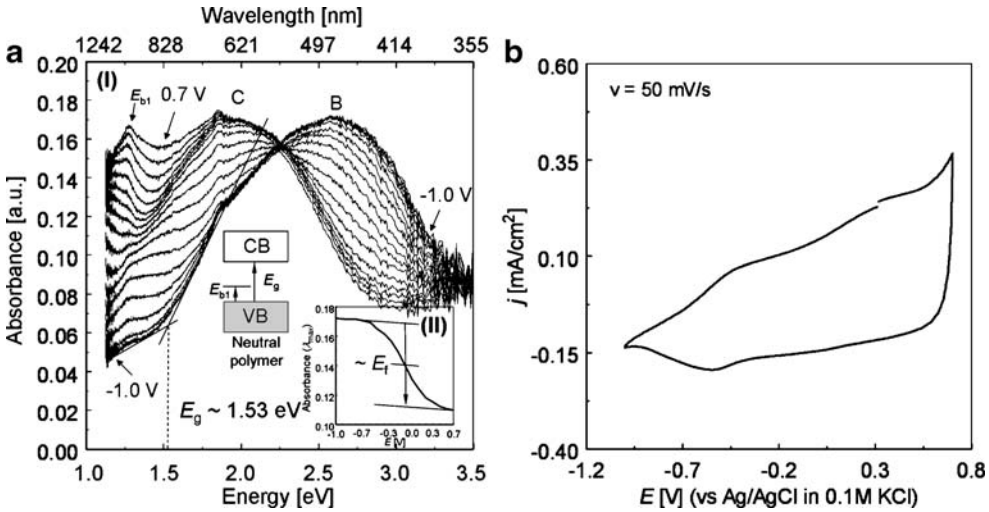

Fig. 3 **a** (*I*) UV-Vis spectra for pEDOT/Cl film in 0.1 M KCl; potential range from –1.0 to 0.7 V, inset (*II*) shows absorbance vs. potential spectra. **b** Cyclic voltammetry curves obtained for ITO/pEDOT/Cl electrode in 0.1 M KCl solutions; sweep rate, 50 mV/s

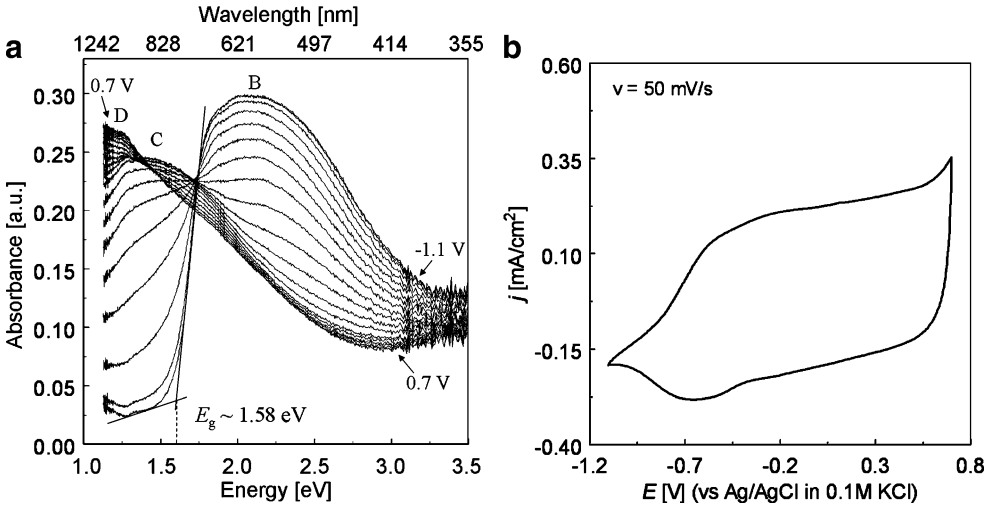

Fig. 4 **a** UV-Vis spectra for pEDOT/PSS film in 0.1 M KCl. **b** Cyclic voltammetry curves obtained for ITO/pEDOT/PSS electrode in 0.1 M KCl solutions; sweep rate, 50 mV/s

polymer as shown in the inset of Fig. 2a (II). The E_f value is equal to −0.2 V.

ITO/pEDOT/Cl

Figure 3a shows UV-Vis spectra of pEDOT/Cl polarized in 0.1 M KCl aqueous electrolyte. Three maxima absorption peaks can be seen: B, C, and E_{b1}.

The maximum absorption B at λ_{max}≈482 nm confirms the presence of the π–π* transition in pEDOT/Cl. The λ_{max}B is shifted towards lower wavelength of about 100 nm in comparison with the pEDOT/FeCN. This shift confirms a counterion influence on the maximum absorption of the π–π* transition. The maximum absorption C is seen at 630 nm. This broad peak is associated to a polymer phase transformation from a neutral to polaronic form.

The positions of intragap states are also allowed to be determined from spectroelectrochemistry [35]. There is a peak E_{b1} that appears at intermediate doping levels. This peak represents energy level above the valence band edge. Maximum absorption of E_{b1} is seen at λ_{max}=970 nm. The band gap E_g=1.53 eV, whereas E_f is equal –0.1 V (see Fig. 2a (II)).

Figure 3b shows cv curve obtained for the material pEDOT/Cl in 0.1 M KCl at a sweep rate 50 mV/s. The shape of the polarization plot is typical for pEDOT films polarized in aqueous electrolytes free from other redox couples [4].

ITO/pEDOT/PSS

Figure 4a shows UV-Vis spectra of pEDOT/PSS film. The spectroelectrochemical measurements show that the maximum absorption (B) of the π–π* transition is seen at λ_{max}≈ 600 nm. Upon doping, the π–π* transition decreases at the expense (C) of transition at higher wavelength at about 850 nm and "overdoped" phase is formed (D). Łapkowski and Proń obtained similar results for the pEDOT/PSS modified ITO electrode [4].

The band gap energy, determined by extrapolating the onset of the π–π* transition (see Fig. 4a) is equal 1.58 eV which is

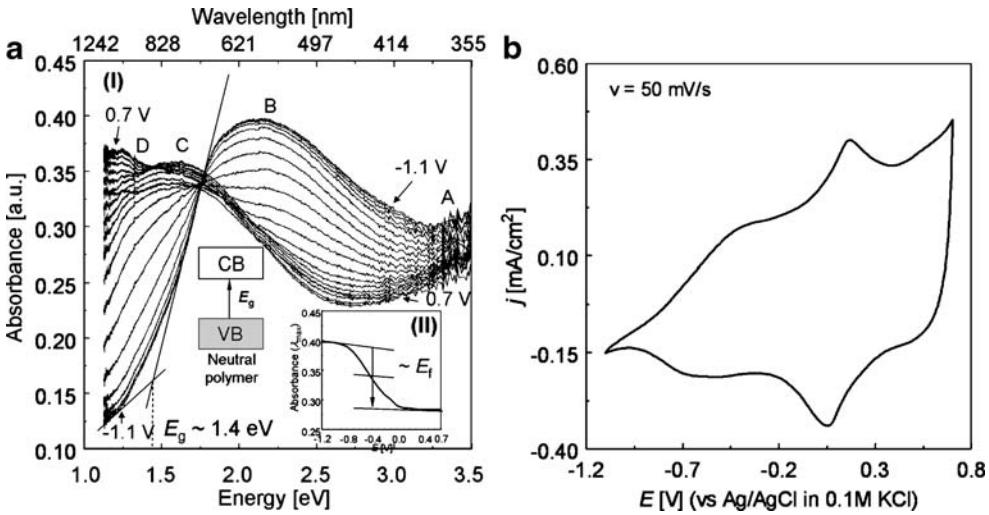

Fig. 5 **a** (*I*) UV-Vis spectra for pEDOT/Fehcf film in 0.1 M KCl; potential range from –1.1 to 0.7 V, inset (*II*) shows absorbance vs. potential spectra. **b** Cyclic voltammetry curves obtained for ITO/pEDOT/Fehcf electrode in 0.1 M KCl solutions; sweep rate, 50 mV/s

slightly different than the values reported for pEDOT films in nonaqueous electrolytes (1.6–1.7 eV) [4, 33, 36].

The E_f value calculated from the absorbance vs. potential data at λ_{max}B (not shown) is equal to –0.4 V and is lower than for pEDOT/FeCN and pEDOT/Cl.

Figure 4b represents cyclic volammetry curve obtained for ITO/PEDOT/PSS electrode polarized with the sweep rate of 50 mV/s in 0.1 M KCl solution. Typical box-shape curve identifies pseudo-faradaic current of polymeric electrode.

ITO/pEDOT/Fehcf

Figure 5a (I) shows UV-Vis spectra of pEDOT/Fehcf obtained in 0.1 M KCl solution. Depending on the potential, the three maxima can be seen: B, C, and D.

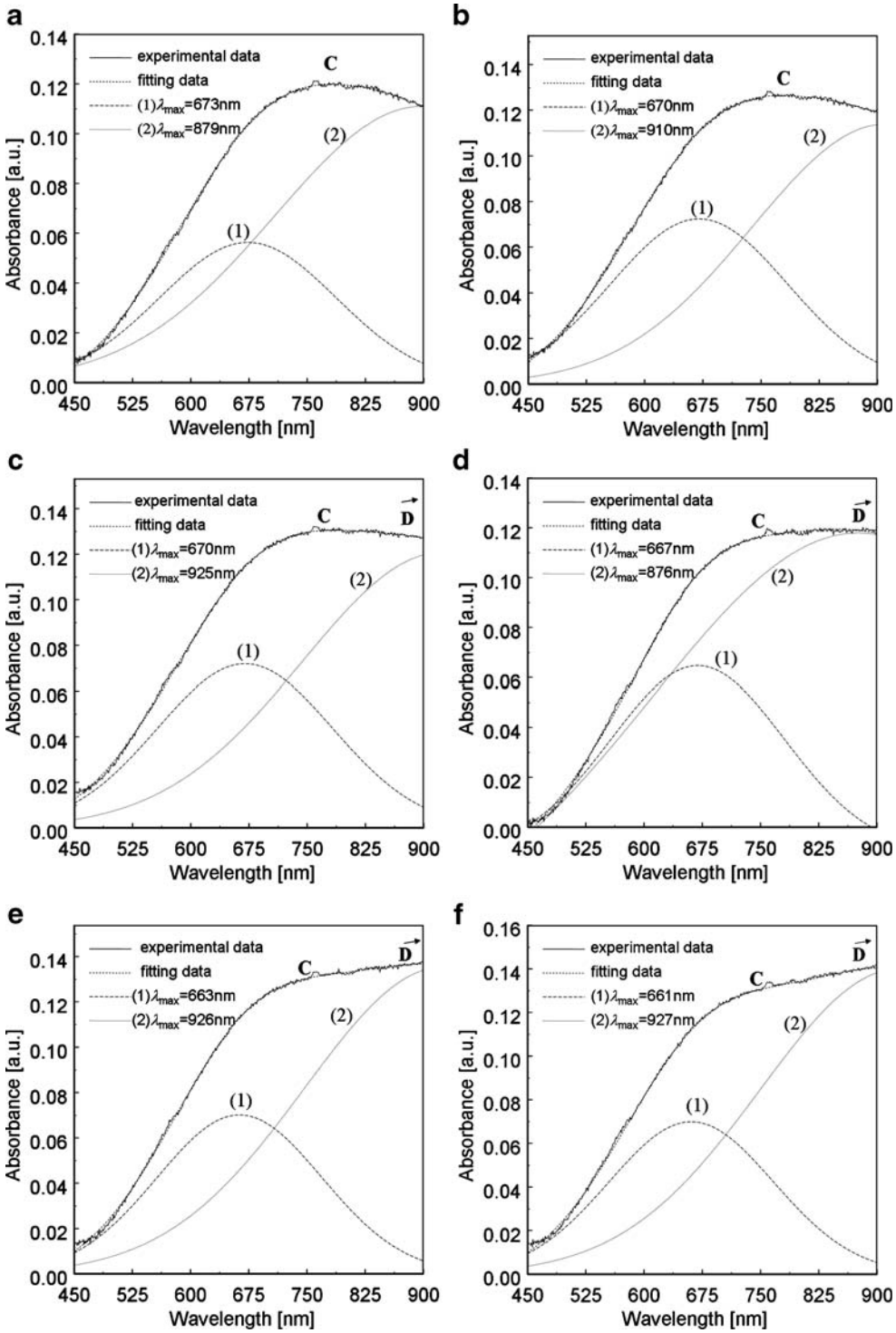

Fig. 6 Mathematical analysis of the UV-Vis spectra for pEDOT/Fehcf as a function of a potential; **a** E=0.2 V, **b** E=0.3 V, **c** E=0.4 V, **d** E=0.5 V, **e** E=0.6 V, **f** E=0.7 V

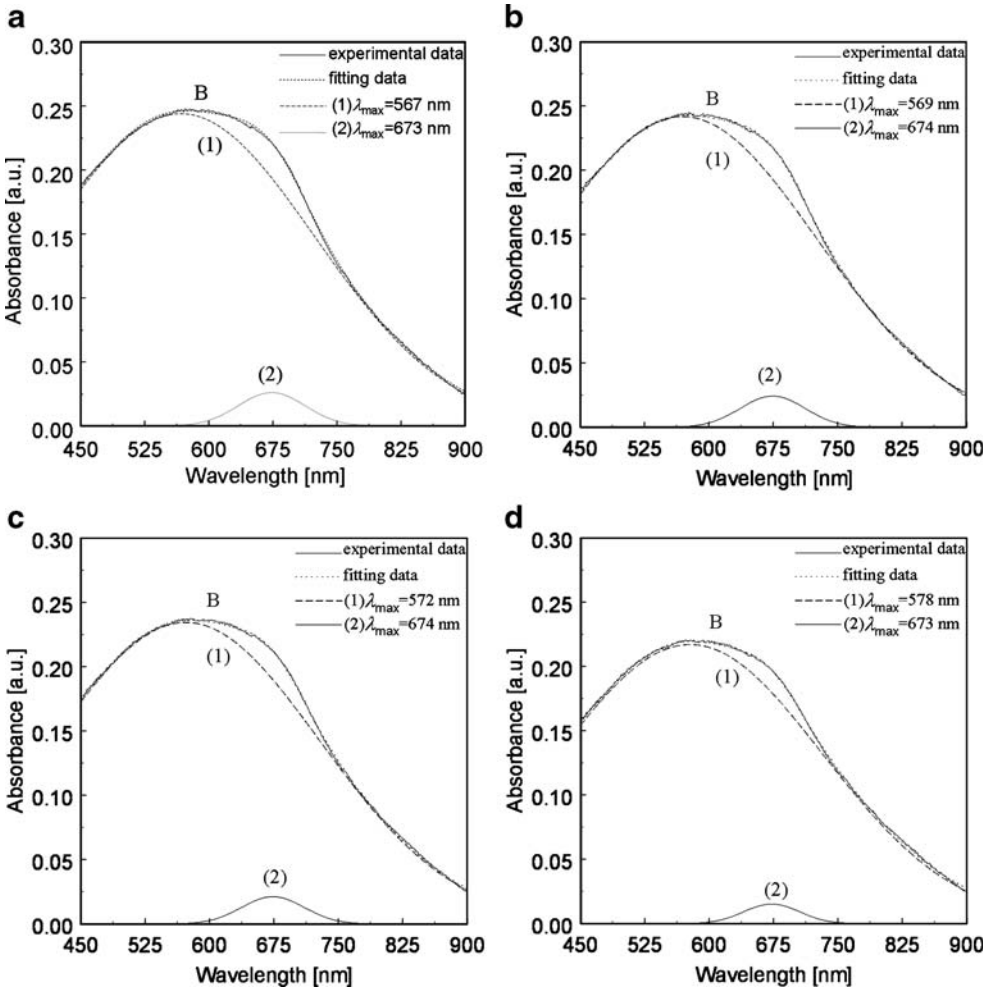

Fig. 7 Mathematical analysis of the UV-Vis spectra for pEDOT/Fehcf as a function of a potential; **a** E=−1.1 V, **b** E=−1.0 V, **c** E=−0.9 V, **d** E=−0.8 V

Moreover, below 400 nm for the whole potential range rinsing absorption curve A is observed. This part of an absorption curve is very likely associated to LMCT in $Fe(CN)_6^{3-}$ forming solid iron hexacyanoferrate (Fehcf) [26, 27].

The maximum absorption at 585 nm (λ_{max}B) confirms the π–π* transition in the composite film. The energy band gap E_g is estimated to be equal 1.40 eV and is lower than for the pEDOT/FeCN. The formal potential of pEDOT/Fehcf is E_f=–0.45 V.

A further anodic polarization of the electrode causes doping process of the pEDOT/Fehcf film. The maximum absorption at λ_{max}B decreases, and new broad peak absorption intensity (C) increases. This λ_{max}C is related to change oxidation state from the neutral to oxidized polymer state. On the UV-Vis spectra obtained at potentials higher than 0.3 V, new maximum (D) is formed (similarly as for pEDOT/FeCN). This maximum is assigned to the transformation of the polaron into bipolaron states [4, 6].

Figure 5b shows cyclic voltammetry curve obtained for ITO/PEDOT/Fehcf electrode polarized with the sweep rate of 50 mV/s in 0.1 M KCl solution. This is typical polarization curve disclosing valence change of high-spin iron atom in Fehcf (about 0.1 V).

It is well known that pure inorganic Fehcf depending on the valence state of metal atom centers exhibits different colors. In reduced state, Fehcf is transparent, in semi-oxidized state is blue, and in full oxidized state is green [36–38] or yellow [39].

On the basis of that knowledge, a mathematical analysis was performed for the maximum absorption C in the potential range from 0.2 to 0.7 V. Program GRAMS/32 4.01 was used for the analysis. The UV-Vis spectra in the range from 450 to 900 nm were analyzed for all studied films. As an example, mathematical analysis for pEDOT/Fehcf is shown in Fig. 6a–f. In that region, one may see the

Table 1 The energy gap E_g estimated for pEDOT/X electrode materials

Electrode material	E_g [eV]
pEDOT/Fehcf	1.40
pEDOT/FeCN	1.55
pEDOT/Cl	1.53
pEDOT/PSS	1.58

π–π* transitions in polymer [27, 29–32] and metal–metal charge transfer (MMCT) in Fehcf [37, 38]:

$$Fe^{3+}\left[Fe^{II}(CN)_6\right]^{4-} \xrightarrow{h\upsilon} Fe^{2+}\left[Fe^{III}(CN)_6\right]^{3-} \quad (1)$$

Figure 6a–f shows mathematical analysis results obtained from spectra of pEDOT/Fehcf with deconvoluted curves. The analysis shows the presence of line 1 with the wavelength maximum in the range from 660 to 670 nm and line 2 with the wavelength maximum above 870 nm. Calculated maxima depend on the potential of the electrode, and they change from 673 nm for 0.2 V to 661 nm for 0.7 V. The second peak is seen at wavelength above 880 nm. The first peak may confirm MMCT in iron hexacyanoferrates present in polymer matrix whereas the second peak proves appearance of an overdoped form of the polymer state.

The mathematical fitting procedure was used also for the reference materials, pEDOT/FeCN, pEDOT/PSS, and pEDOT/Cl. In all cases, during polarization of the modified electrodes in the range from 0.2 to 0.7 V, fitting gave also two maxima. First was localized at about 700 nm and did not change significantly with the electrode potential and the second above 950 nm. Thus, one may conclude that the presence of the peak maximum at 700 nm is not related to metal–metal charge transfer in Prussian blue presented in pEDOT/Fehcf. The second maximum at about 950 nm runs out the analyzed region (from 450 to 900 nm). Hence, one may interpret it as polaron–bipolaron transitions.

The mathematical fitting procedure was also used for neutral state of the polymer for pEDOT/Fehcf (see Fig. 7a–d) and the other polymeric films (not shown).

One may see that, in the range from –1.1 to –0.8 V, two maxima are present. The first peak maximum is seen at about λ_{max}=570 nm. An origin of the peak is related to the π–π* transition in pEDOT [25, 28–33]. The presence of the low peak at λ_{max}≈673 nm may be interpreted as an appearance of inorganic Prussian blue. However, it is known that, in the studied potential range, iron hexacyanoferrate is white (Everitt salt) [28]. Thus, one may conclude that peak at λ_{max}≈673 nm is rather related to the polymer π–π* transitions in pEDOT than MMCT in Fehcf. Low absorbance intensity of line (2) may be caused by the presence of oligomers within the film. Analogous results were obtained for pEDOT/FeCN and pEDOT/PSS (not shown). The presence of the maximum (1) at about 570 nm confirms the π–π* transitions in pEDOT film. The absence of Prussian blue in pEDOT/FeCN and pEDOT/PSS excludes the metal–metal charge transfer coming from Fehcf. Thus, the presence of maximum (2) seems to be associated with the oligomers which were produced during anodic polymerization of the monomer and were trapped as isolated small patches within porous ITO electrode.

Conclusions

Spectroelectrochemical properties of pEDOT/Fehcf, pEDOT/FeCN, pEDOT/Cl, and pEDOT/PSS are dominated by polymer components. The pEDOT/Fehcf and pEDOT/FeCN films exhibit absorption at wavelength below 400 nm in the UV-Vis spectrum which is very likely related to ligand metal charge transfer.

The π–π* transition in pEDOT, excluding pEDOT/Cl film, was ascribed at wavelength≈590 nm. The composition of the polymer film affects strongly the electronic stage of the material. It was shown that formation of the inorganic iron hexacyanoferrate within polymer matrix causes diminishing of the energy band gap in comparison with the other studied materials. The E_g values were 1.40 for pEDOT/Fehcf, 1.55 eV for pEDOT/FeCN, 1.53 eV for pEDOT/Cl, and 1.58 eV for pEDOT/PSS (Table 1). Thus, the synergetic effect between pEDOT and Fehcf is now shown as measured value of the transition from valence to conduction band. As far as we are aware, the E_g 1.40 eV is the lowest value reported for pEDOT films.

Acknowledgments Financial support from Gdansk University of Technology (DS 014668/003) is gratefully acknowledged.

References

1. Dietrich M, Heinze J, Heywang G, Jonas F (1994) J Electroanal Chem 369:87–92
2. Sakmeche N, Aaron JJ, Fall M, Aeiyach S, Jouini M, Lacroix JC, Lacaze PC (1996) Chem Commun 24:2723–2724
3. Kulesza PJ, Miecznikowski K, Chojak M, Malik MA, Zamponi S, Marassi R (2001) Electrochim Acta 46:4371–4378
4. Łapkowski M, Proń A (2000) Synth Met 110:79–83
5. Chen X, Inganäs O (1996) J Phys Chem 100:15202–15206
6. Damlin P, Kavarnström C, Ivaska A (2004) J Electroanal Chem 570:113–122
7. Morvant MC, Reynolds JR (1998) Synth Met 92:57–61
8. Pei Q, Zuccarello G, Ahlskog M, Inganas O (1994) Polymer (Guildf) 35:1347–1351
9. Ren X, Pickup PG (1993) J Phys Chem 97:5356–5362
10. Ogura K, Endo N, Nakayama M, Ootsuka H (1995) J Electrochem Soc 142:4046–4032
11. Koncki R, Wolfbeis OS (1998) Anal Chem 70:2544–2550
12. Noël V, Randriamahazaka H, Chevrot C (2000) J Electroanal Chem 489:46–54
13. Qi Z, Pickup PG (1997) Chem Mater 9:2934–2939
14. Neff VD (1978) J Electrochem Soc 125:886–887
15. Itaya K, Uchida I, Neff VD (1986) Acc Chem Res 19:162–168
16. Mortimer RJ, Rosseinsky DR (1983) J Electroanal Chem 234:133–143
17. Cataldi TRI, Salvi AM, Centonze D, Sabbatini L (1994) J Electroanal Chem 406:91–99
18. Zadronecki M, Wrona PK, Galus Z (1999) J Electrochem Soc 146:620–627
19. Lisowska-Oleksiak A, Nowak AP (2008) Solid State Ionics 179:72–78

20. Sasca V, Stefanescu M, Popa A (2003) J Therm Anal Calorim 72:311–322
21. De Azevedo WM, De Mattos IL, Navarro M (2006) J Mater Sci Mater Electron 17:367–371
22. Al-Yusufy FA, Bruckenstein S, Schlindwein WS (2007) J Solid State Electrochem 11:1263–1268
23. Lisowska-Oleksiak A, Nowak AP (2005) Patent Application P.378023
24. Lisowska-Oleksiak A, Nowak AP (2007) J Power Sources 173:829–836
25. López-Palacios J, Heras A, Colina Á, Ruiz V (2004) Electrochim Acta 49:1027–1033
26. Ayers JB, Waggoner WH (1971) J Inorg Nucl Chem 33:721–733
27. Itaya K, Ataka T, Toshima S (1982) J Am Chem Soc 104:4767–4772
28. Gray HB, Beach NA (1963) J Am Chem Soc 85:2922–2927
29. Kim BY, Cho MS, Kim YS, Son Y, Lee Y (2005) Synth Met 153:149–152
30. Yamato H, Kai K, Ohwa M, Wernet W, Matsumura M (1997) Electrochim Acta 42:2517–2523
31. Cutler CA, Bouguettaya M, Reynolds JR (2002) Adv Mater 14:684–688
32. Sonmez G, Schottland P, Reynolds JR (2005) Synth Met 155:130–137
33. Pacios R, Marcilla R, Pozo-Gonzalo C, Pomposo JA, Grande H, Aizpurua J, Mecerreyes D (2007) J Nanosci Nanotechnol 7:2938–2941
34. Hoffmann R (1987) Angew Chem Int Ed Engl 26:846–878
35. Thomas CA (2002) Ph.D. thesis, University of Florida
36. Zhang D, Wang K, Sun D, Xia X, Chen H (2003) J Solid State Electrochem 7:561–566
37. Pyrasch M, Tieke B (2001) Langmuir 17:7706–7709
38. Rosseinsky DR, Lim H, Zhang X, Jiang H, Chai JW (2002) Chem Commun (Camb) 24:2988–2989
39. Kulesza PJ, Zamponi S, Malik MA, Miecznikowski K, Berrettoni M, Marassi R (1997) J Solid State Electrochem 1:88–93